Numerical Analysis of Granular Soil-Structure Interface Behavior at Large Shearing Displacement: Evolution and Characterization

Babak Ebrahimian [1,2], Ali Noorzad [1]

1- Faculty of Civil, Water and Environmental Engineering, Abbaspour School of Engineering, Shahid Beheshti University (SBU), Tehran, Iran

2- The Highest Prestigious Scientific and Professional National Foundation, Iran's National Elites Foundation (INEF), Tehran, Iran

Emails: ebrahimian.babak@gmail.com; b_ebrahimian@sbu.ac.ir

Abstract

This paper presents the interface behavior between cohesionless granular soil and moving bounding structure using finite element method and a micro-polar elasto-plastic continuum model. The focus of investigation is on the consideration of rough, medium rough and relatively smooth interfaces. In this regard, plane monotonic shearing of an infinite extended narrow granular soil layer between two parallel rigid boundaries of varying surface roughness is simulated under the conditions of constant vertical pressure and free dilatancy. To describe the essential mechanical properties of granular soil, an elasto-plastic single hardening soil model enhanced by polar quantities i.e., Cosserat rotations, curvatures, and couple stresses is employed. Furthermore, the mean grain diameter as the material characteristic length is implemented in the model to properly predict the thickness of shear band formed along the interface as well as to consider the scale effect in the simulations. Particular attention is paid to the influence of boundary condition on the shear behavior of granular soil layer. In this regard, the additional micro-polar kinematical boundary conditions along the boundaries allow more detailed description of the surface roughness of adjoining structure. It is shown that the assumed boundary conditions have strong influences on the granular soil behavior in terms shear band thickness and mobilized interface friction angle. For large shearing, the shear deformations and polar quantities are localized within a narrow zone, called shear band, parallel to the direction of shearing and the state quantities tend towards a stationary state. It is also revealed that the location of shear bands is different in an infinite or finite shear layer.

Keywords: Micro-polar continuum, elasto-plasticity, interface shearing, granular soil, finite element.

1. INTRODUCTION

The serviceability of a wide range of engineering structures involving interfaces between their structural elements and adjoining soil bodies is highly dependent on the behavior of soil layer forming close to the surface of bounding structure. Due to the shear movement of bounding structure, the intense shear deformations are localized within the interface, in the form of an induced single shear band [1]. The localized shearing mechanism mainly governs the interface behavior and controls the overall performance of structure having interaction with the soil body [2]. The investigations of soil-structure interface behavior have attracted great attentions of many researchers in recent years. Field observations, laboratory experiments and numerical simulations have been conducted in order to gain insights into the complex phenomena occurred in the soil bodies close to the surface of bounding structures. In this regard, the development of strain localization and shear banding occurring along the interface and the relevant micro-mechanical mechanisms are still not fully known. Most of the previous studies on interface behavior between granular media and rough surfaces have focused on exploring and quantifying factors influencing peak and steady state strength along the interface [3-9]. However, very limited experimental works have been published on shear deformation of interface due to difficulty in collecting microscopic information, at the scale of soil grains, interior to the soil samples [10-11].

In this paper, shear behavior of interface between granular soil body and moving bounding structure is analyzed using FEM and micro-polar continuum approach. To this end, a micro-polar elasto-plastic single hardening soil model is applied to simulate the mechanical behavior of cohesionless granular materials like sand [12-13]. Plane monotonic shearing of an infinite long and narrow granular soil layer, located between two parallel rigid boundaries of varying surface roughness, is investigated under constant vertical pressure and free dilatancy. In FE analyses, the emphasis is given to the influence of bounding structure's surface roughness on the shear band thickness as well as the mobilization of shear strength along the interface. Furthermore, the

distribution and evolution of polar quantities and state variables are mainly focused to precisely consider the interface shear behavior of granular soil layer in contact with a bounding structure. Micro-polar kinematical boundary conditions are introduced to describe different roughness values of interface. Such conditions take into account Cosserat rotation, displacement along the boundary, surface roughness of bounding structure, and the ratio between slip and corresponding Cosserat rotation along the boundary. Following the relevant literature, this research presents the first numerical simulation systematically addressing the effect of continuum surface roughness on the shear behavior of neighboring micro-polar elasto-plastic granular material. Furthermore, the numerical results obtained in this study can be considered as a basis to be compared with the future laboratory experiments and DEM-simulations.

2. REVIEW OF CONSTITUTIVE MODEL

Cosserat continuum kinematics are distinguished from classical continuum theory by introducing an extra rotational degree of freedom of a body-point, independent of translational degrees of freedom [14]. For plane strain problems, each material point has three degrees of freedom, two translational represented and one rotational. In Cosserat continuum stress and strain tensors are generally non-symmetric due to the existence of couple stresses and curvatures. According to [14], the objective or Cosserat strain rate tensor now can be redefined as

$$ {}^{n+1}_{n}\dot{\gamma}_{ij} = {}^{n+1}_{n}\dot{E}_{ij} + \left({}^{n}\dot{\Omega}_{ij} - {}^{n}\dot{\Omega}^{c}_{ij} \right) \tag{1} $$

$$ \dot{\Omega}_{ij} = \frac{1}{2}\left(v_{i,j} - v_{j,i} \right) \tag{2} $$

$$ \Omega^{c}_{ij} = -e_{ijk}\omega^{c}_{k} \tag{3} $$

$$ {}^{n}\kappa_{ij} = {}^{n}\omega^{c}_{j,i} \tag{4} $$

where, $\dot{E}_{ij}$ is classical strain-rate tensor; Ω and Ω^c are classical spin and Cosserat spin tensors, respectively; e_{ijk} is the Ricci permutation tensor; and κ_{ij} curvature vector of deformation or the gradient of grain rotation. The single hardening Lade's model enhanced with Cosserat rotations, curvatures and couple stresses [12-13], is used in this study. The model is obtained through extending non-polar Lade constitutive relations [15-17] by Cosserat quantities. Lade's model is an elasto-plastic soil model with single yield surface expressed in terms of stress invariants. The employed micro-polar Lade's model is enhanced through the second stress and deviatoric stress invariants in order to incorporate the material characteristic length. The model formulations are very briefly discussed here to make this paper self-contained and more details are found in [12-13]. The constitutive constants of micro-polar Lade's model can be determined by the simple standard laboratory experiments. The model has totally 16 material constants, for 11 of which (M_L, λ, υ, m, η_1, μ, ψ_2, h, α, C and P) the calibration procedure are conducted based on the experimental data of three conventional CD triaxial tests and one isotropic compression test. These 11 constants are calibrated similarly in both micro- and non- polar version of Lade's model because the micro-polarity is not affected for purely homogeneous and co-axial deformations with zero couple stresses. The definition of material constants and calibration procedure are presented in [12-13]. Non-linear elasticity modulus is as follows:

$$ E = M_L P_a \left[\left(\frac{I_1}{P_a} \right)^2 + \left(6\frac{1+\upsilon}{1-2\upsilon} \right) \frac{J_2'}{P_a^2} \right]^{\lambda} \tag{5} $$

where, P_a is a reference pressure used for normalizing the stress invariants (this pressure is assumed as atmospheric pressure); I_1 is the first invariant of stress tensor ($I_1 = \sigma_{ii}$,; where, i = 1, 2, 3); M_L and λ are dimensionless material parameters, determined by a series of simple experiments of loading–unloading–reloading cycles (for more details see [15]); υ is constant Poisson's ratio; and J_2' is the second invariant of deviatoric stress tensor according to [14]. The mentioned invariant is enhanced to account for the couple stress effect and expressed as:

$$J_2' = \left\{ \left[\left(\sigma_{11}-\sigma_{22}\right)^2 + \left(\sigma_{33}-\sigma_{22}\right)^2 + \left(\sigma_{11}-\sigma_{33}\right)^2 \right] + \left(\frac{\sigma_{12}+\sigma_{21}}{2} \right)^2 \right\} + \frac{\left(m_1^2+m_2^2\right)}{l^2} \tag{6}$$

where, σ_{ij} and m_i are stress and couple stress, respectively; and l is the internal length scale.
The second invariant has been enhanced to incorporate the effect of couple stresses (m_i) and expressed as follows:

$$I_{II} = \frac{1}{2}\left(\sigma_{12}\sigma_{21} - \sigma_{11}\sigma_{22} - \sigma_{11}\sigma_{33} - \sigma_{22}\sigma_{33}\right) - \frac{m_1 m_2}{l^2} \tag{7}$$

Stress tensor is expressed in the 2D Cosserat continuum in the vector form as follows:

$$\{\sigma\} = \left\{ \sigma_{11} \quad \sigma_{22} \quad \sigma_{33} \quad \sigma_{12} \quad \sigma_{21} \quad m_1/l \quad m_2/l \right\}^T \quad or \quad \{\Sigma\} = \begin{Bmatrix} \sigma \\ \mu \end{Bmatrix} \tag{8}$$

Similarly, the objective strain vector, including strain and curvature of rotations, is non-symmetric and defined as:

$$\{\gamma\} = \{\nabla U\} = \left\{ \gamma_{11} \quad \gamma_{22} \quad \gamma_{33} \quad \gamma_{12} \quad \gamma_{21} \quad l\kappa_1 \quad l\kappa_2 \right\}^T \quad or \quad \{\gamma\} = \begin{Bmatrix} \varepsilon \\ \kappa \end{Bmatrix} \tag{9}$$

In FE implementation, each node has the following degrees of freedom in the plane strain Cosserat continuum as:

$$\{U\} = \left\{ u_1 \quad u_2 \quad \omega_3^c \right\}^T \tag{10}$$

The following constitutive law can be used:

$$\{\dot{\sigma}\} = [D]\{\dot{\gamma}\} \tag{11}$$

where, [D] is elasto-plastic stiffness matrix.

A quadrilateral isoparametric 4-node element is used in this study. Gaussian integration technique [18] has been applied to achieve numerical integration of surface and volumetric integrands. Static equilibrium equations are fulfilled using Newton-Raphson method. In this investigation, the proposed micro-polar Lade's single hardening model is implemented into a non-linear FE program in order to investigate the interface shear behavior between granular soil and bounding structure under motion.

3. MODELING INTERFACE BEHAVIOR

The interface behavior between granular soil layer and bounding structure under large shearing movement is investigated using finite element method. In this regard, a section of lateral infinite extended narrow granular soil layer located between two parallel rigid boundaries of varying surface roughness is considered under free dilatancy and constant vertical pressure (Figure 1). The granular layer is modeled with the proposed micro-polar elasto-plastic Lade's model described in Section 2. The prescribed interface conditions are related to the surface roughness of top and bottom boundaries and the properties of granular medium. Apart from stress and displacement boundary conditions of non-polar conventional continuum, additional non-standard micro-polar kinematical boundary conditions, i.e. couple stress and Cosserat rotation, must also be introduced along the boundaries of Cosserat granular layer.

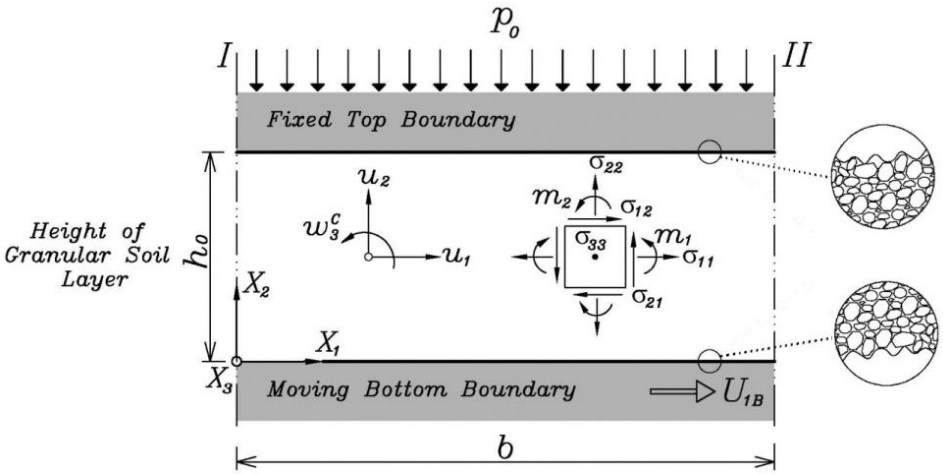

Figure 1. Modeling plane shearing of granular material under constant vertical pressure: section of extended infinite granular soil layer located between two parallel rigid boundaries of varying surface roughness along with kinematics and static quantities of micro-polar material under plane strain condition

In this study, the relation proposed by Tejchman (1997) [1] is used between Cosserat rotation and shear displacement at the top and bottom boundaries of granular soil layer to describe the interface behavior:

$$\omega_3^c = -f\, u_{1B}/d_{50} \tag{12}$$

The above kinematic boundary condition is proposed in the form of a constant ratio of Cosserat rotation to the displacement, occurred along the top and bottom boundaries of layer, to describe different roughness values. In fact, Cosserat boundary conditions allow different boundary roughnesses with considering grain rotations. The interface coefficient (*f*) depends on the interaction between soil grains and boundaries. The dimensionless factor (*f*) denotes u_{1B} fraction, transmitted to the soil grains in the form of rotation. This factor can determine the behavior of interface between granulate and surface of bounding structure. In the numerical calculations, presented in this paper, different values are chosen for the interface coefficient to account for the influence of surface roughness of top and bottom boundaries on the shear behavior of granular soil layer. The calculations are performed for rough, medium rough and relatively smooth interfaces. In the following, it is assumed that relatively smoother bounding interface is corresponded to a higher value of *f*. In fact, smooth interface shear behavior is observed when boundary soil grains are large relative to any counterface topography. On the other hand, full shearing of the material is assumed ($\omega_3^c = 0$) along a rigid surface for modeling very rough interfaces [12]. A slip occurs along a very rough surface if the surface friction angle reaches its residual value with no simultaneous deformation [19]. Up to this point, the material experiences shearing. It is noted that the shear displacement (u_{1B}) can be viewed as a relative displacement between top and bottom boundaries. Therefore, a similar proportional relation is assigned to Cosserat rotation on the top and bottom surfaces. In the present FE calculations, the proportional relation given in Equation (12) is described for the rates of Cosserat rotation (micro-curvature), on the bottom and top surfaces, and applied shear displacement (displacement gradient) and presented as follows:

$$x_2 = 0: \qquad \dot{\omega}_{3B}^c = -f_B \frac{\dot{u}_{1B}}{d_{50}} \tag{13}$$

$$x_2 = h: \qquad \dot{\omega}_{3T}^c = -f_T \frac{\dot{u}_{1B}}{d_{50}} \tag{14}$$

where, f_B and f_T are interface coefficients reflecting the interface conditions between surface grains and boundaries at the bottom and top surfaces of granular soil layer, respectively. In the above relations, *h* represents the thickness of soil layer; d_{50} is the characteristic length of granular soil; where h >> d_{50} is assumed so that the top boundary of granular soil layer has little influence on the formation of shear band along the bottom boundary.

In this study, all calculations are performed for a shear layer with an initial height of h_0 = 4 *cm* and the width of *b* = 10 *cm* and starting from same homogeneous and isotropic states: initial void ratio (e_0) = 0.6; initial

pressure (p_0) = 100 *kPa* ; stresses (σ_{ij}) = $P_0 I$; and couple stresses (m_i) = 0. The mentioned boundary conditions also imply zero assumption of shear stresses and couple stresses in the initial state. The layer is discretized by 4-node elements, each with the dimensions of 1.25 *mm* × 1.25 *mm*. Particularly, the boundary conditions assumed along the top and bottom surfaces of granular soil layer are:

$$u_1(x_1,0)=u_{1B},\ u_2(x_1,0)=0,\ \omega_3^c(x_1,0)=\omega_{3B}^c$$

$$u_1(x_1,h)=0,\ u_2(x_1,h)=u_2(x_1+\Delta x_1,h),\ \omega_3^c(x_1,h)=\omega_{3T}^c,\ \sigma_{22}(x_1,h)=-p_0=-100\,kPa$$

The vertical displacements of top surface of granular soil layer are obtained as a result of dilatancy or contractancy behavior within the whole layer. A vertical pressure of p_0 = 100 *kPa* is kept constant at the top surface. Therefore, the initial height of shear layer is not kept constant during shearing and can changes as the result of dilatancy or contractancy of material under shearing. Along the bottom boundary (x_2 = 0), the vertical displacement (u_2) is zero and the applied horizontal displacement is the same for bounding structure (U_{1B}) and bottom surface of granular layer (u_{1B}). This assumption implies that the possibility of relative displacement, resulted from lower skin frictions, is not considered along the surface of bounding structure [19]. A shear deformation is initiated by applying horizontal node displacements (U_{1B} = u_{1B}). The material behavior to be described is rate independent; therefore, time increment can be related, for instance, to the increment of initiated shear displacement. The calculations are performed for large deformations using an Updated Lagrangian formulation. The symmetry condition of a lateral infinite extended narrow granular soil layer can be modeled by applying constraint conditions to the side nodes of its FE mesh. It means that each node on the left boundary is controlled to have the same displacements and Cosserat rotation as the corresponding node with the same vertical coordinate on the right boundary [12-13]. Therefore, the numerical results are independent of horizontal coordinate as well as the width of FE mesh. Regarding the infinite shear layer, the field quantities are independent of coordinate in the shearing direction with respect to the coordinate system, shown in Figure 1. Field quantities are also independent of the coordinate x_3 in the plane strain condition. Kinematic quantities are displacements (u_1 and u_2) and micro-rotation (Cosserat rotation, ω_3^c); and non-zero static quantities are stress components (σ_{11}, σ_{22}, σ_{33}, σ_{12}, σ_{21}) and couple stress components (m_1, m_2) in the plane strain conditions, concerning Cartesian coordinate system, Figure 1. The calibrated material constants given in Table 1, for a dense silica sand [12-13], are used in numerical simulations of subsequent sections.

Table 1- Lade's model parameters for dense silica sand

Elastic properties			Failure criterion		Plastic potential		Yield criterion		Yield criterion	
M_L	λ	υ	m	η_1	μ	ψ_2	h	α	C	P
292.6	0.25	0.13	0.37	84.1	2.2	-3.06	0.95	0.3	7e-5	2.6

This paper presents the influence of interface condition (various interface roughness values) between granular soil layer and moving bounding structure on the shear behavior of layer. The distribution and evolution of state variables and polar quantities are proposed for the first time for an infinite elasto-plastic micro-polar shear layer in contact with a continuum of different surface roughness values. This issue is studied here under large shear displacements to precisely investigate the interface shear behavior of granular soil. Special attention is paid to rough, medium rough and relatively smooth interfaces under pure translatoric motion. The effects of rotation resistance of soil grains are studied in the form of various surface roughness values along the interface, considering three different micro-polar kinematical boundary conditions (*Cases* 1-3). The descriptions of their surface roughness values are summarized in Table 2. The results obtained from numerical simulations of these cases are presented and discussed in the following. The cases, called *Case* (1) to (3), give a representative collection of interface condition for granular soil layer in contact with rigid boundaries of various surface roughness values at the top and bottom surfaces of soil layer.

Table 2- Description of surface roughness in different simulated cases

Case	Boundary Condition along Top Surface	Top Surface Roughness Description	Boundary Condition along Bottom Surface	Bottom Surface Roughness Description
1	f_T = 0	very rough	f_B = 0.0001	rough
2	f_T = 0	very rough	f_B = 0.01	medium rough
3	f_T = 0	very rough	f_B = 0.5	relatively smooth

4. NUMERICAL RESULTS AND DISCUSSIONS

In *Cases* 1-3, locked Cosserat or micro-rotations have been assumed along the top surface of shear layer in order to model a very rough surface condition [12]. While a certain coupling between Cosserat rotation and horizontal displacement of bounding structure is assumed along the bottom surface of layer indicating rough, medium rough or relatively smooth interfaces. Therefore, micro-polar boundary conditions are non-symmetric in the entire layer for the mentioned cases.

The distribution of normalized horizontal and vertical displacements (u_1/h_0, u_2/h_0), and void ratio (e) across the normalized height of infinite granular soil layer (x_2/d_{50}) is plotted in Figure 2. Unlike earlier investigations of the authors for very rough surfaces along the bottom and top boundaries of granular soil layer [12], in *Cases* 1-3, the location of shear band deviates from the middle of shear layer for rough, medium rough and relatively smooth interfaces. For very rough surfaces, no grain sliding and rotating may occur along the bottom and top boundaries of layer. Thus, the resulting shear localization is within a narrow zone in the middle of layer for large shearing. This implies that the location of localized deformations significantly depends on f values, representing the surface roughness of top and bottom boundaries. According to Figure 2(a), the horizontal displacement gradient close to the interface decreases as f increases. In *Cases* 1-3, as the bottom surface roughness decreases which corresponds to higher values of f_B , the horizontal displacement of granular soil layer relative to the bounding structure is limited to a narrower zone near the bottom bounding structure. Then, the displacement decreases rapidly with increasing its distance from the structure. In the mentioned cases, u_1/h_0 is approaching to zero at the parts farther from the bounding structure or interface. In *Case* 1 (rough bottom interface: $f_T = 0$ and $f_B = 0.0001$), shear band is located near the middle of layer. In *Case* 3 (relatively smooth bottom interface: $f_T = 0$ and $f_B = 0.5$), it is formed along the bottom adjacent to the moving boundary of soil layer with the thickness of about $2d_{50}$, confirmed by the experiments [1]. Unlike non-polar continuum, in the proposed micro-polar continuum approach the normalized horizontal displacement field (u_1/h_0) across x_2/d_{50} is no longer linear from the beginning of shearing, Figure 2. The deformations are inhomogeneous from the beginning of shearing, Figure 2. The distribution of displacement field (u_1/h_0, u_2/h_0) varies significantly within the layer as f_T and f_B increase, Figure 2(a,b). According to Figure 2(A), the surfaces with higher roughness which can fully mobilize the granular soil strength will develop the thickest shear bands (e.g., *Case* 1: $f_T = 0$ and $f_B = 0.0001$). The surfaces with lower roughness will sustain a lower stress ratios (e.g., *Case* 5: $f_T = f_B = 0.1$) and accordingly, develop the shear bands with lower intensity and thickness, Figure 2(C). The higher and lower values of void ratio (e) are obtained within and outside the shear band, respectively, Figure 2(c). Void ratio significantly increases within the shear band. Maximum void ratio values increase in the shear band as U_{1B}/h_0 increases. As f increases, the zone of higher void ratio moves from the middle of layer towards the bottom interface, Figure 2(c). The distribution of quantities across the height of shear layer is strongly affected by the interface behavior between granular soil layer and bounding structure, Figure 2. According to Figure 2, the location and evolution of shear band strongly pertain to the magnitude of interface coefficients (f_T and f_B) or surface roughness described along the top and bottom surfaces of layer. It seems that the granular soil behavior in the narrow layer is drastically affected by the rotation resistance of soil grains along the interface. According to [1], the interface behavior is significantly affected by the boundary conditions of entire system. This fact is confirmed by this research as well. According to the mentioned figure, shear band is closer to the smooth bottom boundary with higher rotation resistance of soil grains comparing to rough bottom boundary with lower rotation resistance.

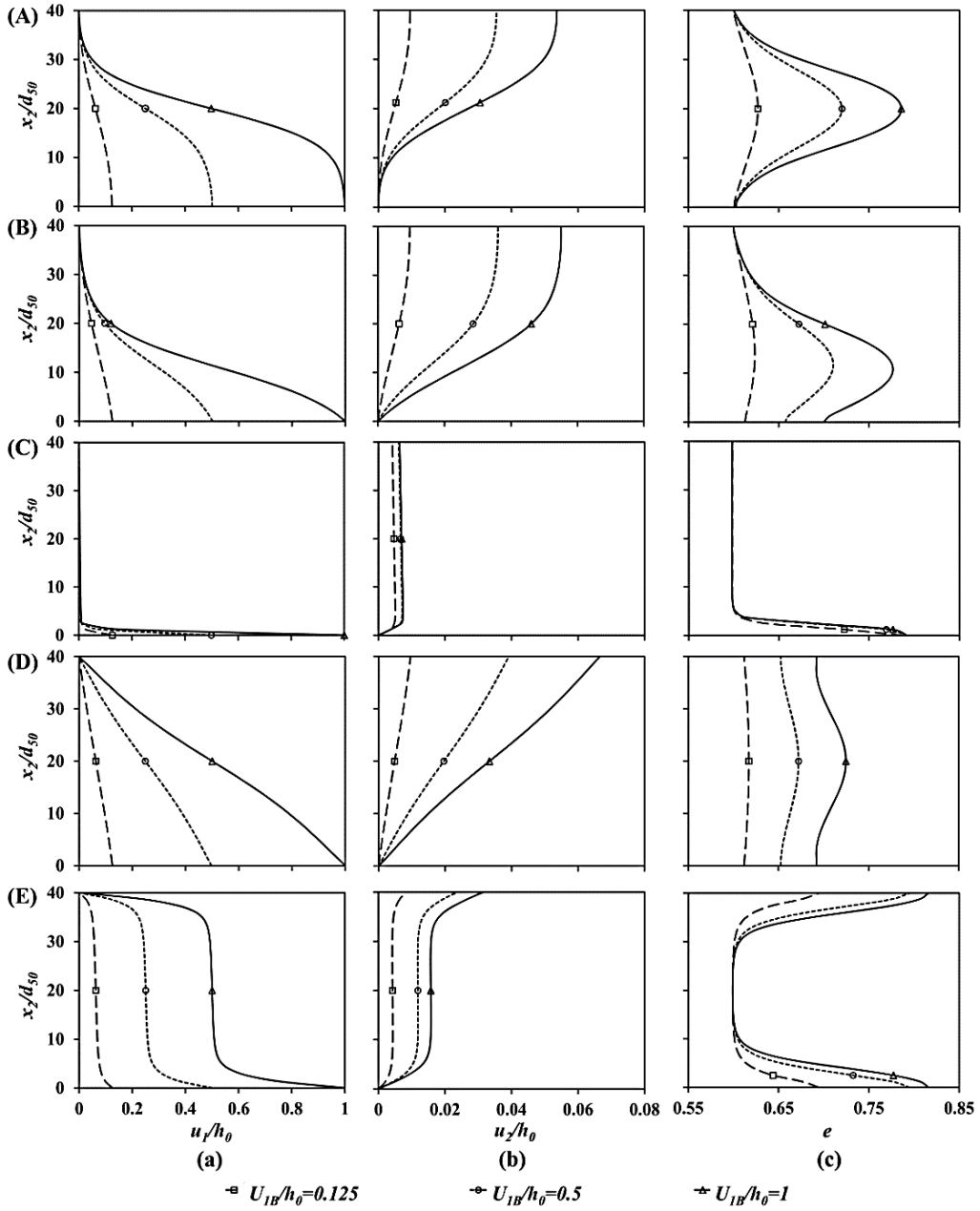

Figure 2. Distribution of (a) u_1/h_0, (b) u_2/h_0 and (c) e across x_2/d_{50} at different U_{1B}/h_0 for: (A) *Case* (1): $f_T = 0$ and $f_B = 0.0001$, (B) *Case* (2): $f_T = 0$ and $f_B = 0.01$ and (C) *Case* (3): $f_T = 0$ and $f_B = 0.5$

Figure 3 shows the profile of Cosserat rotation (ω_3^c), normalized micro-curvature ($\kappa_2^* = l.\kappa_2, (l = d_{50})$) and normalized couple stress ($m_2^* = m_2/(l.\sigma_{22}), (l = d_{50})$) during shearing across x_2/d_{50}. According to Figure 3(a), Cosserat rotations have high values within the shear band and nearly zero value outside it. As U_{1B}/h_0 and f increase, Cosserat rotation increases inside the shear band while outside shear band these quantities remain almost unchanged. Based on the results obtained from numerical simulations, the zone of strain localization is no longer located in the middle of shear layer, Figure 3(E). These results indicate that the location of shear localization in the granular material can be influenced by the interface behavior as well as the rotation resistance of soil grains in contact with the surface of moving bounding structure. According to Figure 3, the shear bands developed along the surfaces with smaller roughness (*Case* 3) are much thinner than those of greater roughness (*Cases* 1,2). Numerical simulations with different boundary constraints for ω_3^c show that the location and thickness of shear band are influenced by interface conditions between granular medium and boundaries. The interface conditions are related to the surface roughness of boundaries and properties of granular medium. The

thickness of localized zone is lower in *Case* 3 than those of *Cases* 1,2 comparing Figure 3(a-C) with Figure 3(a-A,a-B). The lower the rotation resistance, the closer the localized zone to the bounding structure surface. This result generally shows that shear deformations are concentrated in the areas with large soil grain rotations. Significant grain rotations, accompanied by dilatancy, are observed within the shear band (Figures 2(b,c),3(a)). The development of Cosserat rotation outside the shear band is nearly stopped as shear deformations are localized. High Cosserat rotation, manifested in shear band, is closer to the smooth bottom boundary compared to rough bottom boundary. Shear band thickness is significantly lower in the smooth interfaces, $f_B \geq 0.5$, (about $2d_{50}$), comparing to that of rough interfaces, $f_B \leq 0.0001$, (about $32.5d_{50}$). In turn, the maximum Cosserat rotation is larger and more concentrated (due to the lower shear band thickness) in the smooth interfaces, comparing to that of rough interfaces. Figure 3(b) shows normalized micro-curvatures (κ_1^*, κ_2^*), distributed across x_2/d_{50}. According to this figure, the values of κ_1^* are zero across the height in all magnitudes of U_{1B}/h_0 and f. However, the values of κ_2^* are noticeable in the shear band during shearing and increase as U_{1B}/h_0 and f increase. Oppositely, κ_2^* has extremely lower values approaching to zero outside the shear band. In parts where κ_2^* is nearly zero, the material behaves as a rigid body. The highest values of κ_2^* in the thinnest shear band (around $2d_{50}$ thickness) corresponds to relatively smooth surface condition (i.e., *Case* 3: $f_T = 0$ and $f_B = 0.5$). Fig. 4(c) shows the distribution of normalized couple stress components (m_1^*, m_2^*) across x_2/d_{50}. The values of m_1^* are zero across the height for all magnitudes of U_{1B}/h_0 and f. In general, couple stress and micro-curvature are zero in the middle of shear band, regardless the amount of shearing, Figure 3(b,c). The profile of normalized couple stress (m_2^*) across x_2/d_{50} shows highly non-linear patterns in all cases, Figure 3(c). According to this figure, the distribution of m_2^* changes drastically when f increases. The variation of m_2^* depends significantly on the values of U_{1B}/h_0 and f. For relatively smooth interface condition (*Case* 3: $f_T = 0$ and $f_B = 0.5$), zero values of couple stresses across a large part of layer height correspond to the presumption of classical continuum; i.e. grain rotations (Cosserat rotations) are equal to macro-rotations (continuum rotations). In this case, couple stress (m_2^*) has almost constant values across the height excluding the upper and lower boundaries of soil layer. The sign of normalized couple stresses is switched at the middle of shear band in all magnitudes of U_{1B}/h_0 and f. However, the highest values of normalized couple stress (m_2^*) occur along the interface ($x_2 = 0$) for smooth interfaces ($f_B \geq 0.5$) within a narrow band of $2d_{50}$ thickness.

Figure 4 shows the evolution of normalized normal and shear stress components ($\sigma_{11}^*, \sigma_{22}^*, \sigma_{33}^*, \sigma_{12}^*, \sigma_{21}^*$) as well as mobilized interface friction angle (φ_m) versus normalized horizontal displacement of bounding structure (U_{1B}/h_0) at different positions across x_2/h_{50}. All shear stress-displacement curves first increase up to a peak value higher than the limit shear stress. Then, they are followed by softening and a reduction to a steady state shear stress, Figure 4. The limit resistance is achieved once the stationary state is reached in the shear band. According to this figure, normal stress components approach to same limit value of P_0. The evolution of σ_{12}^* is the same across the height in all elements, while that of σ_{21}^* is different based on the position of elements across the layer height, Figure 4(A). A pronounced difference between σ_{12}^* and σ_{21}^* can be observed after peak. Two stages, characterized as steep increase and then gradual decrease, can be distinguished in Figure 4.

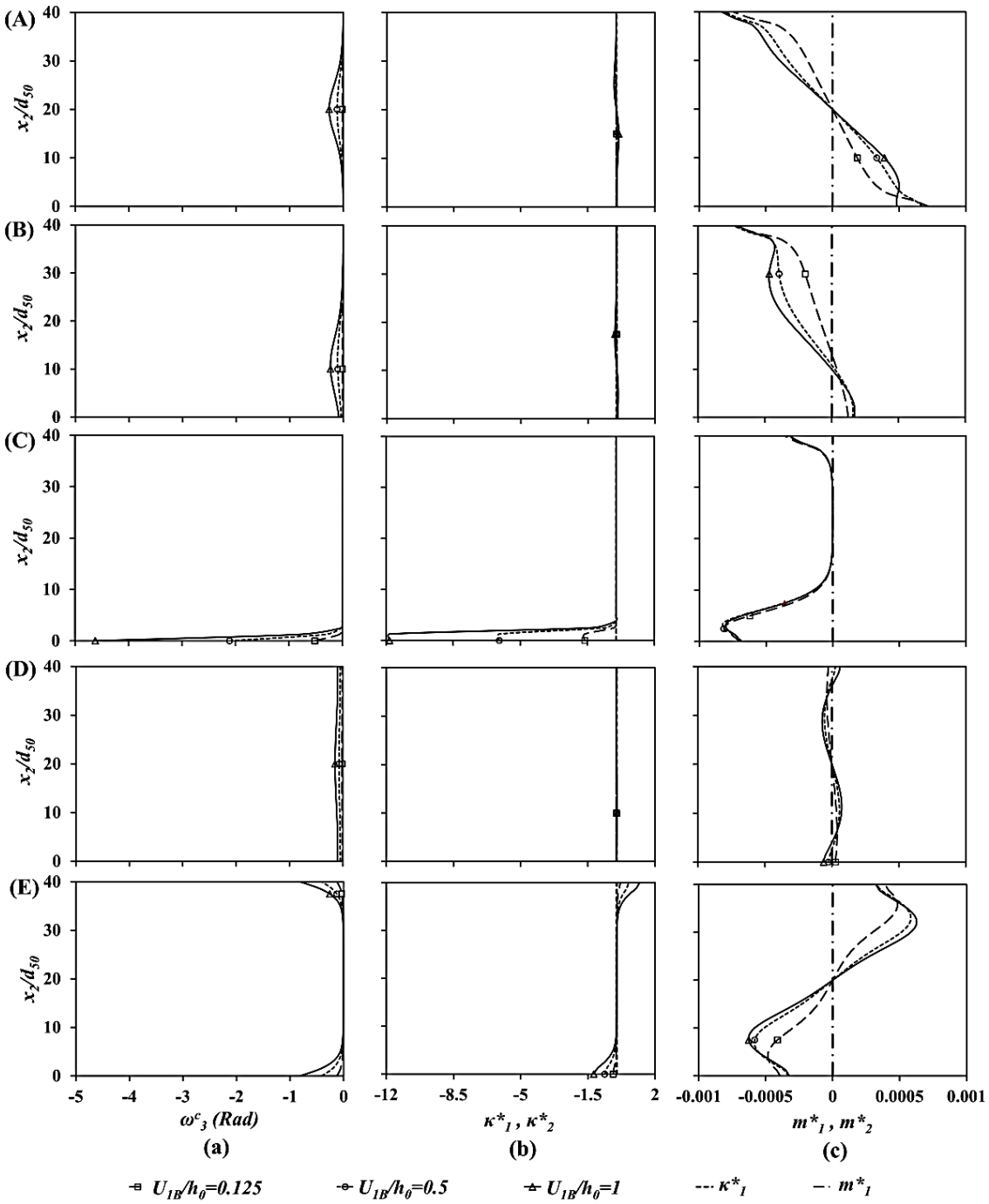

Figure 3. Distribution of (a) ω_3^c , (b) $\kappa_{1,2}^*$ and (c) $m_{1,2}^*$ across x_2/d_{50} at different U_{1B}/h_0 for: (A) *Case* (1): f_T = 0 and f_B = 0.0001, (B) *Case* (2): f_T = 0 and f_B = 0.01 and (C) *Case* (3): f_T = 0 and f_B = 0.5

The interface coefficient (*f*) has a strong influence on the resistance magnitude of bounding structure against shearing. For large displacements of bounding structure, normalized shear stresses tend towards a stationary value which depends on the assumed stress limit condition. As surface roughness increases or *f* decreases, peak and residual shear strengths increase. It is shown in Figure 4 that the surface roughness has a controlling effect on the shear strength along the interface. The rougher interface (e.g., *Case* 1) exhibits a higher strength compared to the smoother interface (e.g., *Case* 3). This is reasonable because the rougher interfaces are more interlocked with the soil grains and thus more resistant to shear, Figure 4(B). Distinct post-peak strain softening to steady state is observed in *Case* 1 (f_T = 0 and f_B = 0.0001) due to the low value of f_B, Figure 4(a). Rough interfaces exhibit post-peak displacement-softening behavior and smooth interfaces approximately post-peak plastic behavior. The yielding of smooth interfaces is almost elastic-perfectly plastic. Figure 4(B) shows

the evolution of mobilized interface friction angle (φ_m) versus normalized horizontal displacement of bounding structure (U_{1B}/h_0). φ_m is related to the entire granular soil layer, as the stresses (σ_{12} and σ_{22}) are constant across the height and along the length of layer. φ_m first goes sharply up towards its peak, and then decreases gradually to meet its stationary value in the shearing under constant vertical pressure, P_0 = 100 *kPa*. The highest peak shear strength is achieved in *Case* 1 when the interface is roughest, Figure 4(B-a).

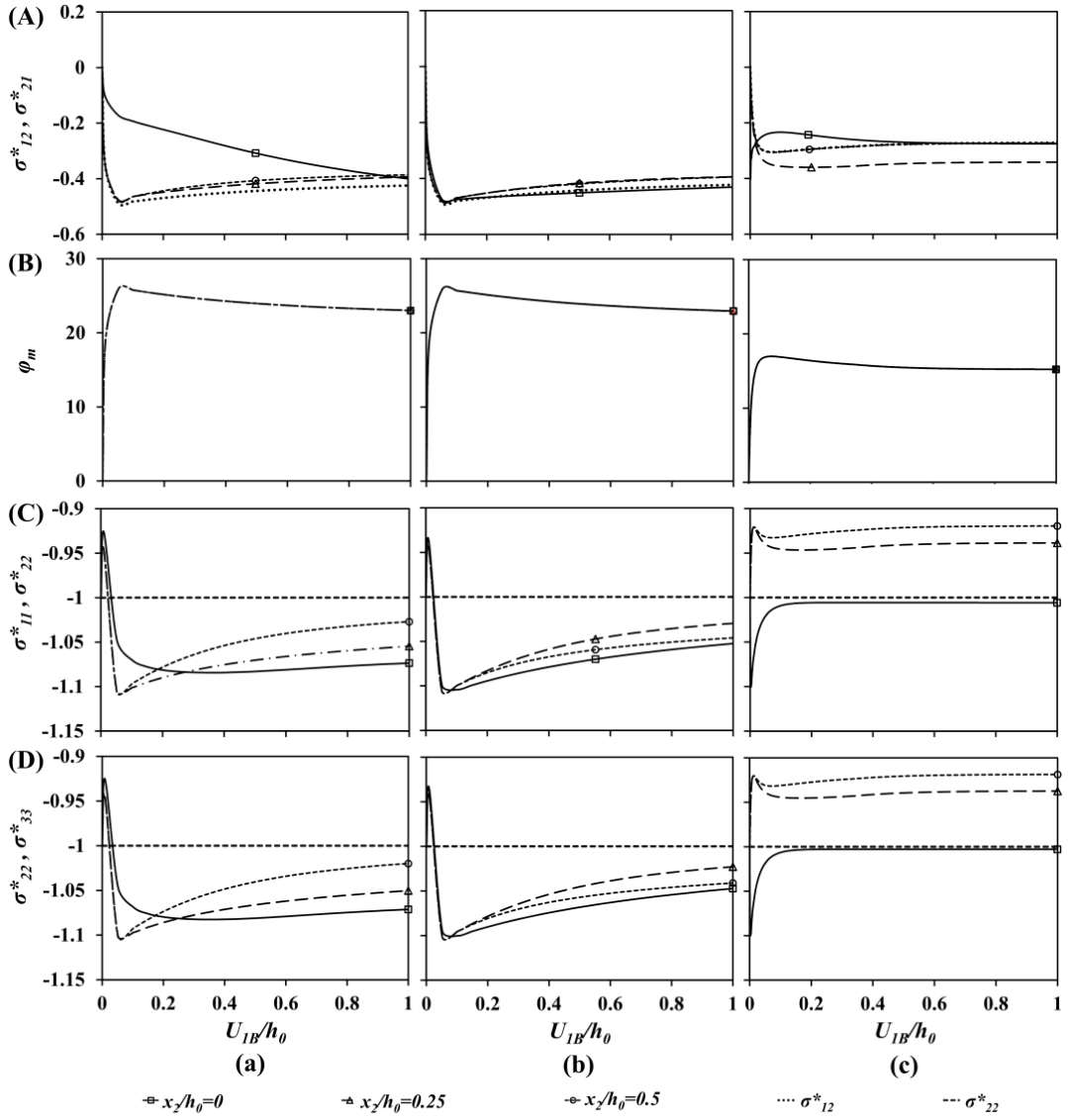

Figure 4. Evolution of (A) $\sigma^*_{12}, \sigma^*_{21}$, (B) φ_m, (C) $\sigma^*_{11}, \sigma^*_{22}$ and (D) $\sigma^*_{22}, \sigma^*_{33}$ at different x_2/h_0 for: (a) *Case* (1): f_T = 0 and f_B = 0.0001, (b) *Case* (2): f_T = 0 and f_B = 0.01 and (c) *Case* (3): f_T = 0 and f_B = 0.5

Considering the quantities of horizontal shear stress (σ^*_{12}), the mobilized peak and residual interface friction angles are φ_m = 26.0˚ and 23.0˚, 25.8˚ and 22.8˚, 16.4˚ and 15.2˚ for *Cases* 1 to 3, respectively, Figure 4(B). Similar to shear stresses, the mobilized interface friction angle (φ_m) also shows a steeply increase phase followed by a very gradual decrease toward stationary value, Figure 4(B). According to this figure, the magnitude of φ_m directly depends on the surface roughness of top and bottom boundaries.

Figure 5 presents the deformed granular soil layer along with the contour plot of void ratio after the horizontal shear displacement of U_{1B}/h_0 = 1.0 for different values of interface roughness (*f*). The brighter zones, in the plots, are corresponded to the higher void ratios or where failure may start. Shear band is fully developed at the steady state, having higher void ratios than other parts of the layer due to the dilation, Figure 5. It is found that the shearing mechanism of granular soil–structure interface is dramatically changed with the magnitude of c*f* . Comparing the deformed configurations, presented in Figure 5, the location and thickness of shear bands depend significantly on the described interface coefficient (*f*) in the form of surface roughness. As *f* increases,

the localized shear deformation zone moves from the middle of layer to the bottom surface of the layer adjacent to bounding structure. Shear band is located in the vicinity of interface in *Case* 3 (f_T = 0 , f_B = 0.0001) and close to the mid-height of soil layer in *Case* 1 (f_T = 0 and f_B = 0.0001). The predicted thicknesses of shear band, derived from the distributions of void ratio and Cosserat rotation, are about $32.5d_{50}$, $25d_{50}$, $2.5d_{50}$ for *Cases* 1 to 3, respectively. Numerical simulations with different boundary constraints for ω_3^c show that the location and thickness of shear band are influenced by the interface conditions between granular medium and boundaries. The interface conditions are related to the surface roughness of boundaries and the properties of granular medium. It is found that boundary effects play significant roles in the interface shear behavior of granular soil.

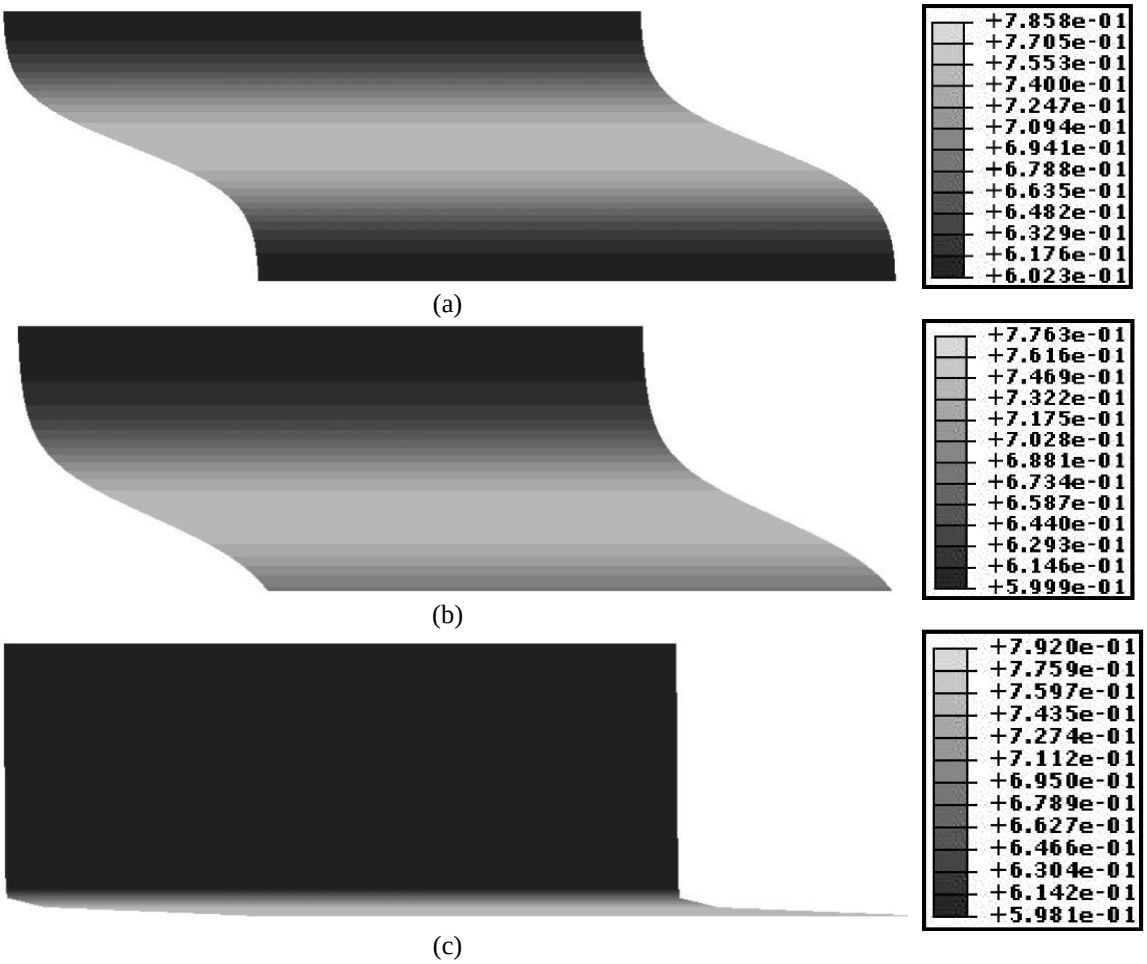

Figure 5. Deformed shape of granular soil layer along with contour plot of void ratio after U_{1B}/h_0 = 1.00 for: (a) *Case* (1): f_T = 0 and f_B = 0.0001, (b) *Case* (2): f_T = 0 and f_B = 0.01 and (c) *Case* (3): f_T = 0 and f_B = 0.5

5. CONCLUSIONS

This paper has quantified how the interface roughness between granular soil layer and rigid bounding structure influences the shear behavior of particulate-continuum interface system. The main findings can be summarized as follows:

- Boundary effects and soil grain rotation resistance are two major factors which influence the response of infinite granular soil layer in contact with bounding structure under plane quasi-static shearing. The results reveal the micro-structural and boundary effects on soil behavior at the very beginning of shearing.
- The pattern, location and thickness of shear band(s) depend on the roughness of top and bottom boundaries, specimen size and boundary conditions of the whole system. Strain localization is formed near the boundary with large Cosserat rotations at the boundary surface. When Cosserat rotations are locked or very small, then the zone of strain localization is formed far away from the boundary. Localized zone occurs in the middle of

shear layer for locked Cosserat rotations along the top and bottom of shear layer. Otherwise, it is located close to the boundary with higher Cosserat rotations. Particularly, if the top or bottom boundaries are smooth, shear band is created directly at the boundaries. If the boundaries are very rough, then shear band occurs in the mid-height of granular soil layer. Regarding rough boundaries, it forms close the mid-height and in medium rough boundaries between the middle and bottom of layer. Shear band thickness, or the zone with intense shear strain, increases with increasing surface roughness or decreasing interface coefficient (*f*). The values of shear band thickness, obtained in this study, are ranged from negligible (1-2d_{50}) for relatively smooth interface up to maximum (32.5d_{50}) for rough interface. As a result, the surfaces with greater roughness generally sustain higher stress ratios and develop thicker shear bands. The most intense shear band with maximum thickness of 32.5d_{50} is developed by the surfaces which can fully mobilize the material strength.

- The effect of interface roughness on the strength mobilized along the interface as well as on the shearing mechanism is taken into account, using additional micro-polar boundary conditions. However, mobilized shear strength along the interface does not only depend on interface roughness and but also on the boundary conditions of the whole system. Mobilized interface friction angle is derived as natural outcome rather than described when using micro-polar boundary conditions; i.e. no special interface element is needed. The peak and residual mobilized interface friction angles decrease with decreasing interface roughness or increasing interface coefficient (*f*). When free dilation is allowed, as in the case of shearing under constant normal pressure, the shear resistance reaches its peak value and then approaches toward stationary status for continuous shearing.

6. ACKNOWLEDGMENT

The first author wants to express his sincere gratitude to the Iran's National Elites Foundation (INEF) for his moral support and encouragement.

7. REFERENCES

1. Tejchman, J. (1997), "*Modelling of shear localisation and autogeneous dynamic effects in granular bodies*", Publication Series of the Institute of Soil and Rock Mechanics, vol. 140, Gudehus, G., Natau, O., (Eds.), Karlsruhe: University Karlsruhe, pp. 1-353.
2. Gudehus, G. (2008), "*Physical Soil Mechanics*", Springer, Heidelberg.
3. Potyondy, J.G. (1961), "*Skin friction between various soils and construction materials*", Géotechnique 2(4), pp. 339–353.
4. Vermeer, P.A. (1983), "*Frictional slip and non-associated plasticity*", Scand. J. Metall. 12, pp. 268–276.
5. Desai, C.S., Zaman, M.M., Lightner, J.G. and Siriwardane, H.J. (1984), "*Thin-layer element for interface and joints*", International Journal for Numerical and Analytical Methods in Geomechanics 8, pp. 19-43.
6. Boulon, M. (1989), "*Basic features of soil structure interface behaviour*", Computers and Geotechnics 7, pp. 115-131.
7. De Gennaro, V. and Frank, R. (2002), "*Elasto-plastic analysis of the interface behaviour between granular media and structure*", Computers and Geotechnics 29(7), pp. 547-572.
8. Hu, L. and Pu, J. (2003), "*Application of damage model for soil-structure interface*", Computers and Geotechnics 30, pp. 165-183.
9. Liu, H., Song, E. and Ling, H.I. (2006), "*Constitutive modeling of soil-structure interface through the concept of critical state soil mechanics*", Mechanics Research Communications 33, pp. 515-531.
10. Zhang, G., Liang, D. and Zhang, J. (2006), "*Image analysis measurement of soil particle movement during a soil-structure interface test*", Computers and Geotechnics 33, pp. 248-259.
11. DeJong, J.T. and Westgate, Z.J. (2009), "*Role of initial state, material properties, and confinement condition on local and global soil-structure interface behavior*", Journal of Geotechnical and Geoenvironmental Engineering ASCE 135(11), pp. 1646-1660.
12. Ebrahimian, B., Noorzad, A. and Alsaleh, M.I. (2012), "*Modeling shear localization along granular soil-structure interfaces using elasto-plastic Cosserat continuum*", International Journal of Solids and Structures 49 , pp. 257–278.
13. Ebrahimian, B., Noorzad, A. and Alsaleh, M.I. (2017), "*Modeling interface shear behavior of granular materials using micro-polar continuum approach*", Continuum Mechanics and Thermodynamics, https://doi.org/10.1007/s00161-017-0588-4.
14. Vardoulakis, I. and Sulem, J. (1995), "*Bifurcation Analysis in Geomechanics", Blackie Academic & Professional* (an imprint of Chapman & Hall): Glasgow, London, U.K.
15. Lade, P.V. and Nelson R.B. (1987), "*Modeling the elastic behavior of granular materials*", International Journal for Numerical and Analytical Methods in Geomechanics 11, pp. 521-542.
16. Lade, P.V. and Kim, M.K. (1988), "*Single hardening plasticity model for frictional materials*", Computers and Geotechnics 6, pp. 13-29.
17. Kim, M.K. and Lade, P.V. (1988), "*Single hardening constitutive model for frictional materials*", Computers and Geotechnics 5, pp. 307-324.
18. Belytschko, T., Liu, W.K. and Moran, B. (2000), "*Nonlinear Finite Elements for Continua and Structure*", John Wiley & Sons, LTD.
19. Ebrahimian, B. and Bauer, E. (2012), "*Numerical simulation of the effect of interface friction of a bounding structure on shear deformation in a granular Soil*", International Journal for Numerical and Analytical Methods in Geomechanics 36(2), pp. 1486-1506.